

Molecular Recognition of Amidines in Water

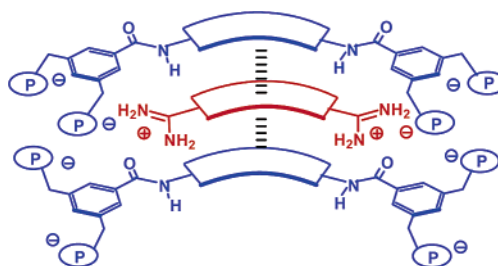
Thomas Grawe, Gerhard Schäfer, and Thomas Schrader*

Fachbereich Chemie, Universität Marburg, Hans-Meerwein-Strasse,
35032 Marburg, Germany

schradet@mailier.uni-marburg.de

Received February 20, 2003

ABSTRACT



Tetraphosphonates of the general structure shown above are biomimetic hosts for bisamidinium cations in drugs such as pentamidine and DAPI. Similar to their insertion into DNA's minor groove, these drugs are often sandwiched by two tetraphosphonate hosts (2:1). The alternative binding mode (1:2) produces extremely high association constants in water of $\sim 10^8 \text{ M}^{-2}$ ($\sim 12 \text{ kcal/mol}$), which can compete with the biological process.

Amidinium cations play an important role in drugs targeting binding pockets for the arginine side chain.¹ By contrast, very few artificial recognition motifs have been found which effectively bind to the amidinium group. The best known is a multicyclic halfmoon-shaped array of annulated pyridine rings and oxime ethers, presented by Bell 10 years ago.² This highly preorganized structure is able to form four linear hydrogen bonds to all NH protons of the amidinium cation in relatively unpolar organic media (Figure 1). Thus, the benzamidinium cation is bound by **1** in 10% methanolic dichloromethane with a K_a value of 10^7 M^{-1} .

We have recently shown that the simple benzylic bisphosphonate **2** recognizes alkyl and aryl guanidinium cations in a chelate fashion with K_a values reaching 10^6 M^{-1} in DMSO.³ We now found that the third guanidinium nitrogen atom can

be replaced by carbon leading to an amidinium species. In a first exploratory experiment, we titrated the *m*-xylylene bisphosphonate **2** with various alkyl and aryl amidinium chlorides in DMSO. Large downfield shifts of the outer and moderate ones of the inner *NH* protons were observed,⁴ in agreement with force-field calculations (Figure 2). We carried out dilution titrations and obtained binding curves which produced an excellent fit with a 1:1 binding model. Nonlinear regression revealed association constants⁵ in the order of 10^5 M^{-1} , 2 orders of magnitude above the classical amidinium phosphonate salt bridge (10^3 M^{-1} in DMSO). Consequently, these simple amidinium–bisphosphonate complexes belong

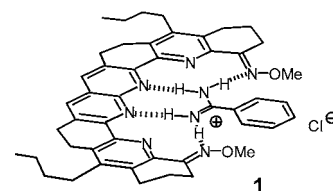


Figure 1. Molecular recognition of benzamidinium chloride by highly preorganized artificial receptor molecule **1**.

(1) Selected examples for thrombin inhibitors: (a) Bode, W.; Turk, D.; Stürzebecher, J. *Eur. J. Biochem.* **1990**, *193*, 175–182. (b) Hilpert, K.; Ackermann, J.; Banner, D. W.; Gast, A.; Gubernator, K.; Hadvary, P.; Labler, L.; Müller, K.; Schmid, G.; Tschopp, T. B.; van de Waterbeemd, H. *J. Med. Chem.* **1994**, *37*, 3889–3901. RGD mimetics: Stilz, H. U.; Guba, W.; Jablonka, B.; Just, M.; Klingler, O.; König, W.; Wehner, V.; Zoller, G. *J. Med. Chem.* **2001**, *44*, 1158–1167.

(2) Bell, T. W.; Santora, V. J. *J. Am. Chem. Soc.* **1992**, *114*, 8300–8302. An imprinted polymer and a dendrimer capable of amidinium recognition have been described: Sellergren, B. *Anal. Chem.* **1994**, *66*, 1578–1582. Zimmerman, S. C.; Wang, Y.; Bharathi, P.; Moore, J. S. *J. Am. Chem. Soc.* **1998**, *120*, 2172–2173.

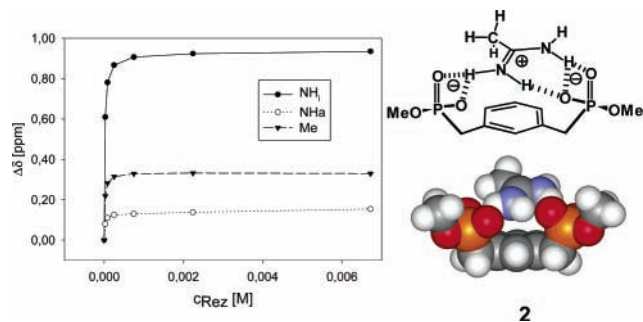


Figure 2. Change in chemical shift of *CH* and *NH* proton signals of acetamide hydrochloride during a typical dilution titration with a 2:1 mixture between host **2** and guest in $[d_6]$ DMSO at 20 °C. Right: Energy-minimized structure of the complex between the acetamidinium ion and bisphosphonate **2**.⁶

to the strongest aggregates known to date for this simple guest species. In pure methanol, the association constants are still on the order of 10^3 M^{-1} . As expected, the introduction of electron-withdrawing substituents in the amidinium's benzene ring enhances its affinity toward the bisphosphonate host (Table 1).

Table 1. Association Constants and Corresponding Gibbs Free Energies from NMR Titrations of Amidinium Chlorides with **2** in DMSO at 20 °C^a

amidinium chloride	$K_{1:1}^b$	ΔG^c	amidinium chloride	$K_{1:1}^b$	ΔG^c
<i>p</i> -methoxy-benz-	7.6×10^4	-6.6	<i>p</i> -amidinium-benzamide	1.4×10^5	-7.0
acet-benz-	1.0×10^5	-6.8	<i>m</i> -nitrobenz-	2.5×10^5	-7.3
	1.2×10^5	-6.9			

^a Due to the strongly hygroscopic character of both titration partners the $[d_6]$ DMSO solution contained ~0.1% of water. Errors in K_a are standard deviations from the nonlinear regressions and were estimated at ± 13 –30%.
^b In M^{-1} . ^c In kcal/mol.

Modern AIDS therapy makes extensive use of bisamidinium salts (against pneumonia): according to detailed binding studies of various research groups the drug pentamidine does not bind by intercalation, but inserts into the minor groove of DNA along the phosphodiester backbone (Figure 3).⁷ The amidinium endgroups are bound by electrostatic interactions with the center of negative charge

(3) Schrader, T. *Chem. Eur. J.* **1997**, *3*, 1537. Schrader, T. *Tetrahedron Lett.* **1998**, *39*, 517–520.

(4) The classical amidinium phosphonate binding pattern uses only the two inner protons of the cationic guest and never gives any shifts of the outer *NH* protons.

(5) Wilcox, C. S. In *Frontiers in Supramolecular Chemistry and Photochemistry*; Schneider, H.-J., Dürr, H., Eds.; VCH: Weinheim, Germany, 1991; p 123.

(6) MacroModel 7.0, Schrödinger Inc.: force-field Amber*, solvent water, 2000 steps.

(7) Edwards, K. J.; Jenkins, T. C.; Neidle, S. *Biochemistry* **1992**, *31*, 7104–7109.

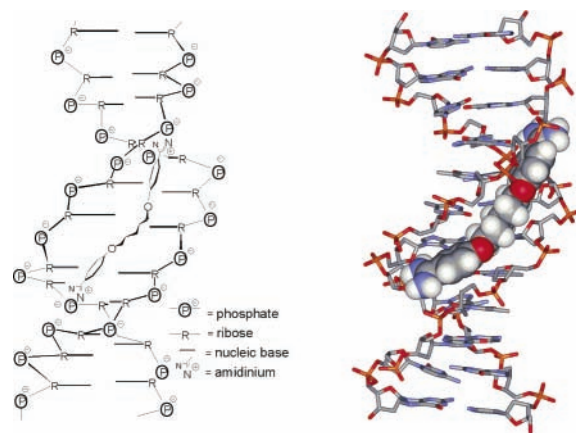
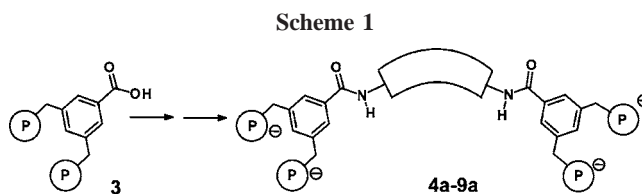


Figure 3. Binding of pentamidine in the minor groove of DNA (ref 8). Right: Modeling structure (MacroModel 7.0, Amber*, water).

density of all phosphate anions, which resides in the interior of the double helix, just above the nucleic bases. The rest of the molecule forms a wide bow in its thermodynamically most favorable form, and thus fits snugly into the curved minor groove.⁸ All other pharmacologically active bisamidines are bound similarly.

We asked ourselves if such a binding mode might be imitated by small model systems. This biomimetic approach could also lead to the first host systems for bisamidinium cations, which might be used for transport, detection, or a controlled release of these drugs. To this end, we synthesized a series of double bisphosphonates, connected by various rigid, semirigid, or flexible spacers of different length. The bisphosphonate-modified benzoic acid **3** was fused with the appropriate α,ω -diamines by standard peptide coupling reagents, and all phosphonic acid diesters were subsequently monodealkylated with LiBr in a dipolar aprotic solvent (Scheme 1).



The tetralithium salts **4a–6a** were dissolved in methanol and titrated with two powerful bisamidinium drugs of different length and flexibility. While pentamidine is relatively long and has a flexible pentyl centerpiece, DAPI (diamidinophenylindole) is much shorter and contains a rigid planar aromatic centerpiece. The results of these binding experiments (all possible combinations were tested) are summarized in Table 2.

Depending on the specific host–guest combination, either clean 1:1 or discrete 2:1 complexes are formed, confirmed

Table 2. Association Constants and Corresponding Gibbs Free Energies ($K_{1:1}$ [M^{-1}] and ($K_{2:1}$) [M^{-2}] from NMR Titrations of Pentamidine and DAPI with **4a–6a** in [d_4]Methanol at 20 °C^a

bisamidinium salt tetrakisphosphonate	pentamidine			DAPI		
	K_a	ΔG^c	stoi. ^b	K_a	ΔG^c	stoi. ^b
<i>m</i> -phenylene 4a	$2 \times 10^5 M^{-1}$	-7.1	1:1	$2 \times 10^5 M^{-1}$	-7.1	1:1
<i>m</i> -xylylene 5a	$4 \times 10^{10} M^{-2}$	-14.2	2:1	$1 \times 10^5 M^{-1}$	-6.7	1:1
<i>p</i> -phenylene 6a	$4 \times 10^{11} M^{-2}$	-15.6	2:1	$1 \times 10^{10} M^{-2}$	-13.4	2:1

^a Errors in K_a are standard deviations from the nonlinear regressions and were estimated at ± 4 –34%. ^b In 2:1 complexes both complexation steps are combined; the ($K_{2:1}$) [M^{-2}] values represent the product of both binary binding constants; the given ΔG values represent the overall free binding enthalpy; for a detailed analysis of each single complexation step see Table 4. ^c In kcal/mol.

by numerous Job plots (Figure 4).⁹ High free energies of binding are found for the 1:1 complexes with K_a values always surpassing $10^5 M^{-1}$.¹⁰ In half of the examined cases,

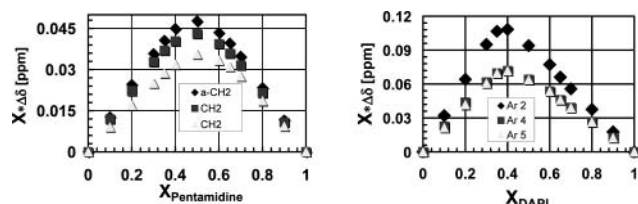


Figure 4. Job plots for complex formation between **4a**@pentamidine (1:1) and **6a**@DAPI (2:1).

two receptor molecules bind to one guest with both association constants in the same range. NMR data and Monte Carlo simulations support the structures shown in Figure 5.

The 2:1 binding mode can be explained only to a small extent with additional electrostatic interactions, especially in view of the excess negative charge of the host molecules. In a dynamic equilibrium, the eight phosphonate arms can be placed around the two amidinium cations so that these are held in the center of their negative charge density. The largest additional attraction, however, most probably originates from hydrophobic and van der Waals interactions which become operative when the second host molecule docks onto the opposite side of the bisamidinium guest.¹¹ These two effects beautifully parallel the binding situation in DNA's minor groove (see above).

(8) (a) Brown, D. G.; Sanderson, M. R.; Garman, E.; Neidle, S. *J. Mol. Biol.* **1992**, 226, 481–490. (b) Laughton, C. A.; Tanious, F.; Nunn, C. M.; Boykin, D. W.; Wildon, W. D.; Neidle, S. *Biochemistry* **1996**, 35, 5655–5661.

(9) Higher aggregates or mixed alternating arrays are highly unlikely, because the Job plots showed maxima close to $X = 0.33$, and sharp signals were always found in the NMR spectra.

(10) The short *m*-phenylene-bridged tetrakisphosphonate **4a** came as a surprise, because it alone formed a 1:1 complex with pentamidine, which is much longer. To recognize both bisphosphonates, the C₅-chain of pentamidine has to twist enormously and form a loop. Since large upfield shifts of all aromatic CH protons indicated a close contact between host and guest, we tried complex formation in pure water and again observed substantial CH shifts of more than 0.2 ppm. Again a definite 1:1 complex was formed with an association constant of $8 \times 10^3 M^{-1}$.

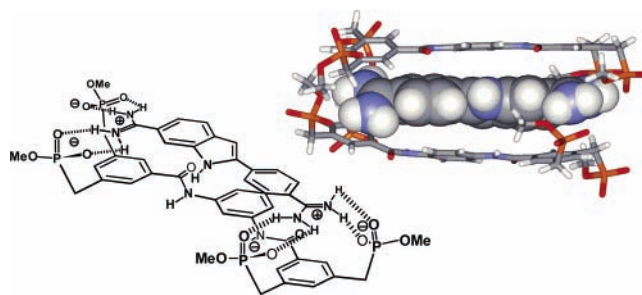


Figure 5. Left: 1:1 complex between tetrakisphosphonate **4a** and DAPI according to Monte Carlo simulations in water (MacroModel 7.0, Amber*, 2000 steps). Right: Lowest energy structure for the 2:1 complex between **6a** and DAPI.

This encouraged us to design tetrakisphosphonates with an optimized distance between their bisphosphonate tips for selective pentamidine and DAPI recognition in water. We synthesized three different host molecules by essentially the same synthetic route as described above. However, this time, all NMR titrations were directly carried out in water; the results are summarized in Table 3.

Table 3. Association Constants and Corresponding Gibbs Free Energies ($K_{1:1}$) [M^{-1}] and ($K_{1:2}$) [M^{-2}] from NMR Titrations of Pentamidine and DAPI with **7a–9a** in D₂O at 20 °C^a

bisamidinium salt tetrakisphosphonate	pentamidine			DAPI		
	K_a^d	ΔG^e	stoi. ^b	K_a	ΔG^e	stoi. ^b
fluorenylene 7a	2×10^4	-5.8 ^c	1:1	$4 \times 10^4 M^{-1}$	-6.2 ^c	1:1
<i>p</i> -xylylene 8a	2×10^4	-5.8	1:1	$7 \times 10^7 M^{-2}$	-10.5	1:2
<i>n</i> -decylene 9a	3×10^4	-6.0	1:1	$5 \times 10^8 M^{-2}$	-11.7	1:2

^a Errors in K_a are standard deviations from the nonlinear regressions and were estimated at ± 6 –28%. ^b In 2:1 complexes both complexation steps are combined; the ($K_{2:1}$) [M^{-2}] values represent the product of both binary binding constants; the given ΔG values represent the overall free binding energy; for a detailed analysis of each single complexation step see Table 4. ^c Due to its low solubility in water, the complexation experiments with **7a** were carried out in a 3:1 DMSO/water mixture.¹² ^d In M^{-1} . ^e In kcal/mol.

Again, high binding energies are calculated, with ΔG values in all cases exceeding $10^4 M^{-1}$. The small decrease in K_a from methanolic to aqueous solution strongly suggests the contribution of substantial solvophobic forces, complemented by van der Waals attractions from the close contact between host and guest faces.¹³ Additional evidence comes from a NOESY experiment in water for the complex between *p*-xylylene tetrakisphosphonate **8a** and DAPI, producing

(11) Table 4 demonstrates the effectiveness of this second step: Usually it equals the first one in free binding enthalpy, only in the case of **6a**@pentamidine and **9a**@DAPI is the first complexation step considerably more exergonic than the second one.

(12) Water solvates the polar headgroups, while DMSO interacts with the nonpolar centerpieces.

(13) Large upfield shifts of aromatic and aliphatic host and guest proton signals of up to 0.4 ppm are produced, especially in water, indicative of dispersive interactions from π -stacking and related processes.

numerous intermolecular NOE cross-peaks between the π -faces of host and guest (Figure 6). In the 1:2 complexes,

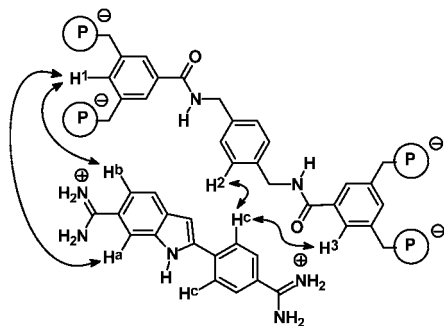


Figure 6. Intermolecular NOE cross-peaks between tetrakisphosphonate **8a** and DAPI in D_2O .

this binding mode leads to a combined binding constant for both complexation steps of up to $5 \times 10^8 M^{-2}$ or ca. -12 kcal mol $^{-1}$. Enzymatic and receptor binding energies are often in this range, and so is DNA's affinity for pentamidine and DAPI (ca. -8 to 11 kcal mol $^{-1}$).¹⁴ To be able to compare our 1:2 complexes with DNA's 1:1 complex, we calculated the amount of bound guest under identical conditions for both hosts (e.g. the same ionic strength etc). The resulting complexation curves are shown in Figure 7. For DNA we

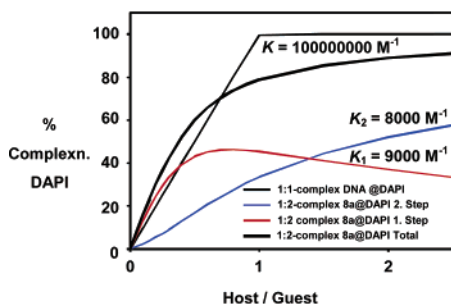


Figure 7. Calculation of the amount of bound DAPI in its 1:2 complex with **8a** and its 1:1 complex with DNA at 10^{-4} M.

assumed an extremely high binding constant of $10^8 M^{-1}$. Despite the much lower K_a values for each single step with **8** ($\sim 10^4 M^{-1}$), the tetrakisphosphonate performs comparably well with DNA up to 75% saturation (solid black line). This means that in the case of an excess of bisamidine our host

(14) Both drugs are moderately AT-selective, rendering their binding constants higher for AT-rich sequences: Cory, M.; Tidwell, R. R.; Fairley, T. A. *J. Med. Chem.* **1992**, *35*, 431–438.

(15) **8a**@DAPI in CD_3OD over both complexation steps: $K_a = 10^9 M^{-2} \sim 12$ kcal/mol.

(16) Eblinger, F.; Schneider, H.-J. *Angew. Chem., Int. Ed.* **1998**, *37*, 826–829. Hossain, M. A. S.; Schneider, H.-J. *Chem. Eur. J.* **1999**, *5*, 1284–1290.

binds about the same amount of DNA. Consequently, both new receptors **8a** and **9a** should be able to interfere with the natural insertion of this bisamidinium drug into the minor groove of DNA.

It makes sense that a perfect complementarity between host and guest invariably leads to the formation of discrete 1:1 complexes, in both methanolic and aqueous solution. However, it is remarkable that an imperfect geometrical fit produces clean 2:1 or 1:2 complexes in most cases. In the 1:2 complexes, high selectivity is reached for one guest, again in both above-mentioned solvents. Thus, *p*-xylylenetetraphosphonate **8a** and *n*-decylenetetraphosphonate **9a** prefer DAPI strongly over pentamidine.

A closer inspection of Tables 2 and 3 reveals that those host molecules which are just a little too short produce 2:1 complexes with their guests, whereas those that are oversized lead to 1:2 complexes. This is not a function of the solvent,

Table 4. Association Constants^a and Corresponding Free Binding Enthalpies K_a [M^{-1}] for Each Single Step of the 2:1 and 1:2 Complex Formation between Pentamidine and DAPI with **5a–9a** in [*d*₄]Methanol or Water^b

bisamidinium salt tetrakis-phosphonate	Step 1		stoi. ^c	Step 2		solv. ^c
	K_a^d	ΔG^e		K_a^d	ΔG^e	
5a @pentam.	2×10^5	-7.1	2:1	2×10^5	-7.1	CD_3OD
6a @pentam.	2×10^6	-8.5	2:1	2×10^5	-7.1	CD_3OD
6a @DAPI	8×10^4	-6.6	2:1	1×10^5	-6.7	CD_3OD
8a @DAPI	9×10^3	-5.3	1:2	8×10^3	-5.2	D_2O
9a @DAPI	1×10^5	-6.7	1:2	5×10^3	-5.0	D_2O

^a HOSTEST 5.60, C. Wilcox, Copyright 1997, University Pittsburgh, USA. ^b Errors in K_a are standard deviations from the nonlinear regressions and were estimated at ± 4 –21%; exception: **9a**@DAPI. ^c See Tables 1 and 2. ^d In M^{-1} . ^e In kcal/mol.

as we could show in the case of **8a**@DAPI: in both methanol and water a clear 1:2 stoichiometry is produced.¹⁵ The critical factor seems to be minimization of electrostatic repulsion between the overhanging ends of hosts or guests.

It remains to be emphasized that in our series of tetrakisphosphonate hosts for bisamidinium guests selectivity does not rely on the flexible or preorganized structure of the linker unit.¹⁶ High affinity for the bisamidinium guest rather results from the favorable combination of electrostatic interactions and solvophobic forces. This might be a new approach to the rational design of highly efficient artificial receptors in water.

We are currently introducing an optical switch in the linker unit, aiming at receptor molecules which can transport drugs to the desired place and release them after a short irradiation with near-UV light.

Supporting Information Available: NMR titration tables and curves, Job plots, structures of host and guest molecules. This material is available free of charge via the Internet at <http://pubs.acs.org>.

OL0343055